Optimal Economic Operation of Microgrids Integrating Wind Farms and Advanced Rail Energy Storage System

Majid Moazzami[1,2]‡, Jalal Moradi[3], Hossein Shahinzadeh[4], Gevork B. Gharehpetian[4], Hasan Mogoei[1]

1- Department of Electrical Engineering, Najafabad Branch, Islamic Azad University, Najafabad, Iran.

2- Smart Microgrid Research Center, Najafabad Branch, Islamic Azad University, Najafabad, Iran.

3- Young Researchers and Elite Club, Khomeinishahr Branch, Islamic Azad University, Khomeinishahr, Isfahan, Iran.

4- Department of Electrical Engineering, Amirkabir University of Technology (Tehran Polytechnic), Tehran, Iran.

(m_moazzami@pel.iaun.ac.ir, sj.moradi@iaukhsh.ac.ir, h.s.shahinzadeh@ieee.org, grptian@aut.ac.ir, hasanmogoei@sel.iaun.ac.ir)

‡ Majid Moazzami; Corresponding Author, Department of Electrical Engineering, Najafabad Branch, Islamic Azad University, Najafabad, Iran, Tel: +98 9133719546, Fax: +98 31442291016, m_moazzami@pel.iaun.ac.ir

Abstract- In this study, an economic model is proposed to simulate the optimal operation of a grid-connected microgrid regard to the uncertainties of microgrids' components. In this study, the wind farms are considered as renewable resources and an innovative technology of advanced rail energy storage (ARES) is deployed as a storage unit. In the optimization model, the stochastic nature of wind energy and the intermittency of loads are contemplated in the model by employing scenario-based Monte Carlo approach to simulate the implication of uncertainties. The objective function of the optimization problem is defined subject to maximize the profit of microgrid's components, and the problem is solved by employing crow search algorithm (CSA). Ultimately, the results of the numerical study are presented and discussed which confirm the effectiveness of the model and appropriate performance of the selected storage technology.

Keywords Optimal Operation, Monte Carlo simulation, Advanced Rail Energy Storage (ARES), Intermittency and Uncertainty, Crow Search Algorithm.

1. Introduction

The exploitation of renewable energy resources is regarded as a lucrative and suitable source of energy for using in the microgrids respect to their small-scale generation capability [1,2]. The microgrids are small-scale power systems that include scattered generation resources and local loads that can operate in two operating modes of connected or disconnected from the upstream network [3-5].

The main challenge in utilizing the renewable resources is the intermittent and uncertain nature of the generated power by these resources [6]. Another major challenge in managing the operation of a microgrid is the uncertainty in the amount of hourly grid consumption caused by the uncertainty in the behaviour of microgrid's users [7]. The microgrids that are connected to the upstream network can participate in the electricity markets and have financial transactions with the upstream network or adjacent microgrids [8]. The microgrids are usually price-taker due to their low generation/consumption capacity compared to the scale of the main network that means they cannot affect the market prices. In this condition, the market price is the uncertainty parameter, and its changes can affect the microgrids' profits [9]. Therefore, extensive studies have been conducted on the optimal operation of microgrids in the presence of the uncertain elements. It is essential to perceive the modelling techniques corresponded with the uncertainty of the volatile elements in the microgrid. In [10], a classification of uncertainty modelling techniques is provided for the renewable resources. In addition, the strengths and weaknesses of these methods are described. The stochastic operation of microgrids is expressed in [11], which is based on the creation of probabilistic scenarios for uncertainty modelling of wind speed, solar radiation intensity, electric loads, and market price. According to the proposed method in this reference, as a mathematical content, the area under the probability density function curve is segregated into sections with different probabilities, and then various scenarios are defined using scenario generation and scenario reduction techniques, which describe different operating conditions. Finally, the optimal operation mode of the microgrid is provided with the accumulation of scenarios. In [12], a stochastic model is proposed to manage the

operation of a microgrid in the next day. The probabilistic operating model proposed by this paper has employed the simultaneous unit commitment and re-dispatch programming of the microgrid to maximize the microgrid's profitability with respect to increase in the wind resources exploitation, as well as minimization of the uncertainty of the consumed electricity. In [13], an optimal operational model is provided for the isolated microgrid considering the uncertainty of the renewable resources and microgrid's loads based on the creation of random scenarios and employment of particle swarm optimization algorithm to solve the problem. The utilized storage technologies in the previous works by other researchers include mainly pumped storage and compressed air energy storage (CAES) technologies. However, these technologies are not practically and economically affordable in the scale of microgrids. In addition, such technologies require specific geological conditions and have environmental restrictions, which deteriorate the possibility of installation of them. Also, the utilization of battery technologies has high operational and maintenance costs. Thus, they are not economically affordable in comparison with the novel technology of advanced rail energy storage (ARES). This technology has also more site availability compared with pumped storage and CAES.

In this paper, an optimal economic operation model for a microgrid which is connected to the upstream network is provided. The model consists of renewable energy sources while the uncertainties, as well as technical and economic constraints, are included. In this model, it is possible to buy/sell power from/to the upstream network. Also, the utilization of an advanced rail energy storage, as a manageable storage unit, plays an influential role in providing a practical model. The contribution of this work is to investigate the impact of the presence of ARES technology in a microgrid, which can be an appropriate alternative in small-scale applications. It is noticeable that, so far, the operational impacts of this storage technology (in power systems and microgrids) have never been addressed in any other similar works. The proposed model has two sections. In the first section, the definite values of the uncertain parameters are obtained by the probability density functions and Monte Carlo simulation. In the Monte Carlo simulation, the mathematical expected value of each uncertain parameter is considered as the definite value of the considered parameter in the optimal operation model. In the following parts, in section two, the microgrid's structure and its components is described. The corresponding equation to wind turbines is represented in this section. In addition, a comprehensive explanation of ARES system is given. The next part of study represents the objective function. The fourth part of the paper deals with mathematical modelling of uncertainties and stochastic contexts. In this section, at first, the Monte Carlo simulation approach is represented. Then the crow search algorithm (CSA) is described to solve the optimization problem. This algorithm is one of the state-of-the-art optimization techniques, which can compete against genetic algorithm and particle swarm optimization algorithm in term of optimization strength and convergence speed. In the section five, the numerical simulation results are presented and discussed. The last part is dedicated to the conclusion.

2. Microgrid Model

The studied microgrid model in this paper is shown in Fig.1. The considered microgrid consists of the wind power unit and ARES series. It is assumed that the ARES series cannot be used simultaneously in the states of charging and discharging. The microgrid is connected at one point to the upstream network, and it exchanges energy with the upstream network through market activities.
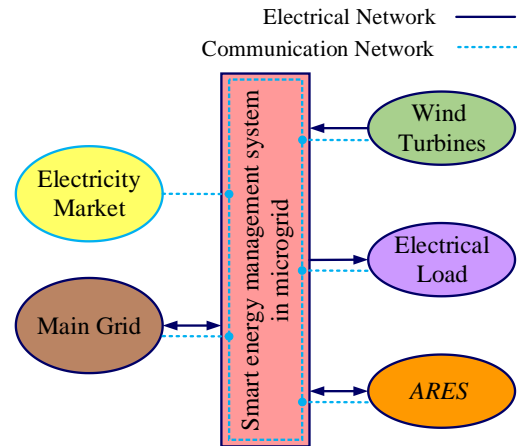

Fig. 1. The studied microgrid model.

2.1. Wind Power Generation

Wind turbine's output power is expressed as a function of wind velocity by Eq. (1):

$$P_{wind}^t(v_t) = \begin{cases} 0 & ,0 \le v_t \le v_{ci}, \ v_{co} < v_t \\ \left(\dfrac{P_{wind}^r}{v_r^3 - v_{ci}^3}\right)v_t^3 - \left(\dfrac{v_{ci}^3}{v_r^3 - v_{ci}^3}\right)P_{wind}^r & ,v_{ci} \le v_t \le v_r \\ P_{wind}^r & ,v_r \le v_t < v_{co} \end{cases} \quad (1)$$

Where $P_{wind}^t(v_t)$ is the wind turbine output power in kW at velocity of v_t. The parameter of v_r is the nominal velocity, and v_{ci} and v_{co} stand for the cut-in and cut-out speeds in m/s respectively. In addition, P_{wind}^r denotes the turbine rated power in kW. The Weibull probability distribution function is used to describe the wind speed uncertainty, which is expressed by Eq. (2). The Weibull distribution has more resiliency and compatibility for simulating the behavior of forecasting errors and inaccuracies compared with normal distribution due to showing skewness and kurtosis.

$$f(v_t) = \frac{k}{c} \cdot \left(\frac{v_t}{c}\right)^{k-1} \cdot \exp\left[\left(\frac{v_t}{c}\right)^k\right] \quad (2)$$

Where k is the shape parameter, and c is the scale parameter. These parameters can be obtained in terms of mean and standard deviation, as shown in Eqs. (3) and (4) [14-16].

$$k = \left(\frac{\sigma_{wind}^t}{\mu_{wind}^t}\right)^{-1.086} \quad (3)$$

$$c = \left(\frac{\mu_{wind}^t}{\Gamma(1 + k^{-1})}\right) \quad (4)$$

2.2. Advanced Rail Energy Storage (ARES)

This innovative technology made up of two large storage yards, which are located at different elevations. These yards are connected to each other by some railway tracks. The track must have a gentle slope to extract the inexhaustible entirely reliable power of gravity. Each yard contains many heavy masses (typically concrete weights), which can be relocated through a specially designed locomotive system. The whole system of locomotive and masses is called a shuttle. A combination of a heavy mass and a locomotive (containing an electrical machine) is called a car. A compact assembly system is designed for masses to minimize the storage area. When a 4-car shuttle descends downhill (discharging process), the electrical machines operate as a generator. In addition, when the masses are raised uphill (charging process), the electrical machines operate as motors. Fig.2. depicts a 1-car shuttle which is manufactured for pilot project and testing purposes [17-19].

Fig. 2. A 1-car shuttle manufactured for testing use [19].

The procedure of storage is similar to pumped hydro technology so that the heavy masses function as water. However, the construction of pumped storage technology is not viable in some power systems because of environmental limitations, site availability restrictions and is not in favour due to being expensive and time-consuming to impound the water by construction of dams, tunnels, and reservoir. Furthermore, the deployment of ARES technology does not need any new technology invention or new science and has a lot of site availability all around the world. This technology can be employed for grid-scale applications and ancillary services. A very advanced control system is implemented for each shuttle to control the procedure of charging and discharging and pickup and drop-off of shuttles. The performance of the whole system depends on the number and the mass of weights, the slope of the tracks, the speed of shuttle-trains as well as the efficiency of electrical machines. This technology can generate electricity within the range of 100 to 3000 MW. The first ARES power plant is designed to generate 668 MW of electricity for connecting to California market. The storage yards have an elevation difference of 3000 ft. There are 5 interconnecting tracks between the yards with the length of approximately 13 km and the slope of approximately 5 degrees. The unit can store 5344 MWh and can be fully discharged within 8 hours. The power plant is

comprised of 140 4-car shuttle units. This plant has the response time of 5 seconds in charging mode and 25 seconds in discharging mode. The storage duration varies from 2 to 24 hours. The time from full charge to full discharge of each shuttle is 34 seconds. It can generally be said that the role of all large-scale storage technology is the same in power system operation and the distinction between them is distinguished by their efficiency (for grid-scale applications). The pumped storage technology, which is the most pervasive storage technology all over the world, usually have the roundtrip efficiency of 65%-80% depending on equipment characteristics, and the most modern PS technologies can reach to the efficiency of 87%. However, the ARES technology can reach the efficiency of 78% in practice. Thus, to what extent ARES technology is better or worse than PS technology depends on the type of PS technology which is compared with. The lifespan of the system is anticipated to be more than 40 years. The high flexibility of this storage system due to the continuous flow of shuttles and its quick-response capability make this storage system appropriate for ancillary services such as frequency control application, var support, voltage regulation, and emergency black-start capability. The ARES technology bridges the gap between large-scale battery and flywheel technologies and highly effective compressed air energy storage and pumped storage technologies as illustrated in Fig.3. In addition, deployment of grid-scale energy storage systems enables more integration of renewable energy resources and helps to smooth their intermittency and volatility. ARES technology can have positive impacts on environmental indices, and reliability and resiliency of the power systems and microgrids.
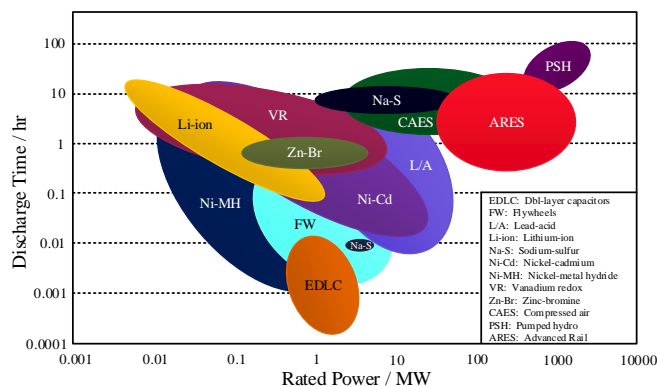

Fig. 3. The comparison of various storage technologies [20].

Shuttle vehicle is the vital part of ARES system. The shuttle system should have the roundtrip of no more than 10% of power losses. The efficiency of the shuttle vehicle is a function of losses due to the motors, inverters, gears, frictions due to wheel slip, and the third rail shoe. A third rail technology is a way of providing electricity to a railway locomotive or a train, through a semi-continuous rigid conductor which are placed alongside or between the rails of a railway track. This method is applied mainly to mass transit or rapid transit systems. By default, the ARES shuttle generates and consumes three-phase 2300 V AC 60 Hz. However, it integrates dual high-efficiency IGBT rectifier/inverters which can deliver the power at the customized level of voltage and frequency. The motor types

are currently available AC traction motors and are axle hung, which is the method used in cutting-edge heavy haul freight diesel–electric locomotive technologies. The powered units of an ARES shuttle vehicle consist of a frame, traction motors, underframe structure, electrical components, air compressor, hydraulic pump, and hydraulic cylinders. The shuttle vehicle has the total weight of 70000 kg for each powered unit and 52000 kg for each unpowered unit and must be able to carry a mass of up to 45 ton.

A large-scale ARES facility approximately will have a capital cost of roughly 1200 \$/kW capacity in comparison with pumped hydro storage facility at 2000–4500 \$/kW capacity, compressed air energy storage at 1800 \$/kW effective capacity, and sodium sulfur batteries at about 3000 \$/kW capacity.

3. Objective Function

The objective function of the microgrid is proposed as below:

$$OF = \max \sum_{t=1}^{t=24} \left[\begin{array}{c} \left((P_{Grid}^t \times \rho_{Grid}^t) + (P_L^t \times \rho_{Sell-load}^t) \times \Delta t \right) \\ - \left(C_{Wind}^t + C_{ARES}^t \right) \end{array} \right] \qquad (5)$$

Where P_{Grid}^t is the exchanged power with the upstream network at t, and $\rho_{Sell-load}^t$ is the price of the sold power to the microgrid's consumers in \$/kWh. t is the length of the time intervals that is equal to one hour. C_{Wind}^t and C_{ARES}^t represent the wind unit and ARES storage unit's costs respectively [12]. The cost of each microgrid's component is the cost of investment, repair and maintenance that is shown in Eq. (6).

$$C = \left(\left(\dfrac{\left(\dfrac{\alpha(1+\alpha)^n}{(1+\alpha)^n - 1} \right) \times A}{CF \times 8760 \times P_{rated}} \times P^t + C_{O\&M} \right) \right) \times \Delta t \qquad (6)$$

Where $C_{O\&M}$ denotes the repair and maintenance cost in \$/h and does not depend on the generated power. CF is the capacity factor, A represents the amount of initial investment in \$, α is the interest rate and n stands for the useful lifespan of the project in terms of year. P^t is the hourly generated or consumed power in terms of kW. The constraints pertaining to the objective function are shown below.

➢ The power balance in the microgrid: The total generated and consumed power in the microgrid at each moment of time must be equal to zero [21-22].

$$P_{grid}^t + P_{wind}^t \pm P_{ARES}^t - P_{Load}^t = 0 \qquad (7)$$

➢ The power transmission capacity for exchanging power with the upstream network is limited to an upper bound.

$$P_{grid}^t \le P_{grid-max} \qquad (8)$$

➢ The charging and discharging capability of ARES is restricted within a bound as follows:

$$P_{ARES-min}^{Charge}(t) \le P_{ARES}^{Charge}(t) \le P_{ARES-max}^{Charge}(t) \qquad (9)$$

$$P_{ARES-min}^{Discharge}(t) \le P_{ARES}^{Discharge}(t) \le P_{ARES-max}^{Discharge}(t) \qquad (10)$$

4. Uncertainty Modelling

4.1. The Model of Electric Load Uncertainty

It is assumed that the data of historical load records of the microgrid, including the mean (μ_L^t) and the standard deviation (σ_L^t) of the microgrid's load pattern are available per hour [23]. The normal probability distribution is used to describe the uncertainty of hourly load of microgrid (P_L^t). Therefore, the microgrid's load probability density function can be obtained from Eq. (11).

$$f_{P_L}(P_L^t) = \dfrac{1}{\sigma_L^t \sqrt{2\pi}} \cdot \exp\left(\dfrac{-(P_L^t - \mu_L^t)^2}{2(\sigma_L^t)^2} \right) \qquad (11)$$

4.2. Electricity Market and Price Uncertainty

The uncertainty in the day-ahead price is described by the normal distribution function as expressed in Eq. (12).

$$f_{P_{grid}}(P_{grid}^t) = \dfrac{1}{\sigma_{grid}^t \sqrt{2\pi}} \cdot \exp\left(\dfrac{-(P_{grid}^t - \mu_{grid}^t)^2}{2(\sigma_{grid}^t)^2} \right) \qquad (12)$$

Where ρ_{grid}^t is the price of exchanged power with the upstream network at time t, and μ_{grid}^t and σ_{grid}^t are the hourly mean and the hourly standard deviation of the price respectively [24].

4.3. Monte Carlo Simulation

Monte Carlo simulation method is employed to model the intermittency of the uncertainties [25]. For example, in this method, firstly the probability density function and cumulative distribution function are obtained using the hourly mean and standard deviation of wind speed data for modelling the wind speed uncertainty. Then by employment of a uniform random number generator, some random numbers are generated which are between zero and one. These random numbers express the probability of wind speeds. The velocities corresponded with these probabilities are obtained by the inverse transformation sampling method. In each iteration of the Monte Carlo simulation, the expected wind speed is equal to the mathematical expected value of all generated samples until the considered iteration, and it is shown as Eq. (13).

$$E(v_t) = \dfrac{\sum_{s=1}^{N} (v_t)^s}{N} \qquad (13)$$

The termination condition in the Monte Carlo simulation is expressed by the coefficient of variance, and it is shown as Eq. (14).

$$COV = \dfrac{\sqrt{\sum_{s=1}^{N} \left((v_t)^s \right)^2 - \left(\dfrac{1}{N} \sum_{s=1}^{N} (v_t)^s \right)^2}}{\sum_{s=1}^{N} (v_t)^s} \qquad (14)$$

If the variance shown in the above equation is lower than a certain limit, the Monte Carlo simulation is converged and the definite amount of wind speed at time t is equal to the mathematical expected value of all generated wind speeds until the considered iteration. If the termination condition is

not materialized, the counter of N will be added by one. This process will be continued to model all the uncertain parameters. The Monte Carlo simulation flowchart is illustrated in Fig.4.
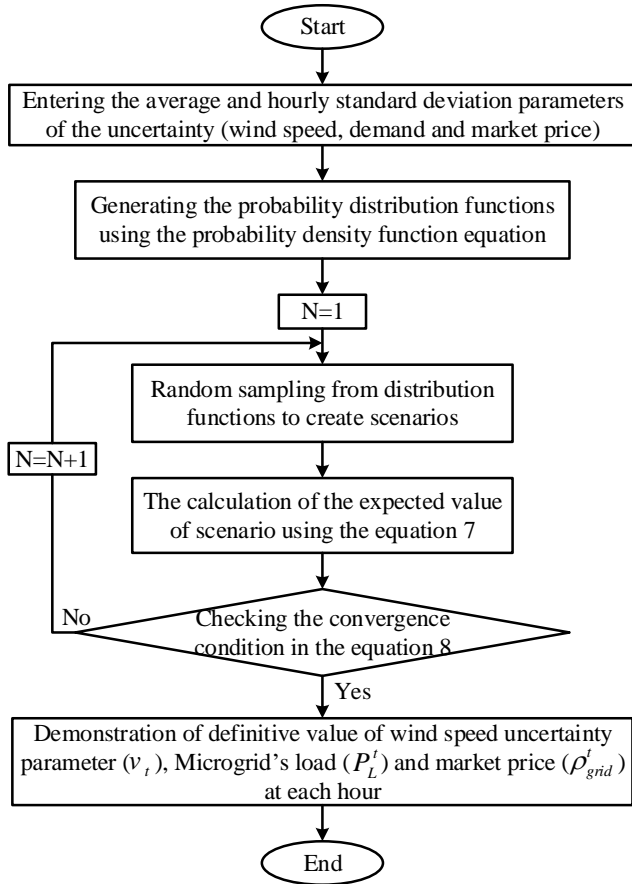

Fig. 4. Monte Carlo simulation flowchart.

5. Crow Search Algorithm (CSA)

Crow search algorithm is inspired from the intelligent behaviour of crows for pilfering other crows' foods and protecting their own food from thievery, which is presented in 2016 [26]. The basics of the CSA algorithm are based on four fundamental behaviours of the crows:

I. Crows live in the flock form,

II. Crows remember the location of their hidden places,

III. Crows follow each other for the purpose of thievery,

IV. Crows protect their caches against the possibility of a being pilfered.

It is assumed that in a *d*-dimensional optimization problem (*d* number of variables), the number of crows is defined by *N*, and the position of the *i*-th crow (answer) in the search space at the moment of *iter* (the iteration) is shown by $X^{i,iter}$. The parameter of $X^{i,iter}$ declares the position of the *i*-th crow while $i=1,...,N$. The range of iteration counter is $iter=1..., iter_{max}$. The $iter_{max}$ is also the highest number of iterations. Each crow has a memory where its hiding location is stored there. At the *iter*-th iteration, the hiding location of the *i*-th crow is shown by $m^{i,iter}$ and it is the best position that the *i*-th crow has been gained so far. In fact, the best

experience has been saved in the memory of each crow. Crows move in the search space to get better positions with more food sources (better hideouts). Suppose that at the *iter*-th iteration, the *j*-th crow wants to fly to its own hiding place defined by $m^{j,ite}$. In this iteration, the *i*-th crow decides to follow the *j*-th crow to reach to its hideout. In this case, two states may occur:

State 1: The *j*-th crow does not know that the *i*-th crow follows it. As a result, the *i*-th crow will reach to the position of the *j*-th crow's hideout. In this state, the new position of the *i*-th crow is obtained by the Eq. (15):

$$X^{i,iter+1} = X^{i,iter} + r_i \times fl^{i,iter} \times (m^{i,iter} - X^{i,iter}) \tag{15}$$

Where r_i is a random number with uniform distribution between zero and one. $fl^{i,iter}$ is the length of the *i*-th crow flying in the *iter*-th iteration. The small values of the *fl* will be led to a local search in the vicinity of $X^{i,iter}$, and its large values will be resulted in a general search far from $X^{i,iter}$.

State 2: The *j*-th crow knows that the *i*-th crow is following it. Therefore, the *j*-th crow flies to another position in the search space to prevent the theft of the *i*-th crow from its hideout. In general, states 1 and 2 can be expressed as Eq. (16).

$$X^{i,iter+1} = \begin{cases} X^{i,iter} + r_i \times fl^{i,iter} \times (m^{i,iter} - X^{i,iter}) & r_j \geq AP^{i,iter} \\ a \quad random \quad position & otherwise \end{cases} \tag{16}$$

```
Randomly initialize the position of a flock of N crows
in the search space
    Evaluate the position of the crows
    Initialize the memory of each crow
    while iter<iter_max
  for i= 1: N (all N crows of the flock)
    Randomly choose one of the crows to follow (for
example j)
    Define an awareness probability
      if r_j≥ AP^{j,iter}
        x^{i,iter+1}= x^{i,iter}+ r_i× fl^{i,iter}×(m^{j,iter} -x^{i,iter})
      else
        x^{i,iter+1} = a random position of search space
      end if
  end for
    Check the feasibility of new positions
    Evaluate the new position of the crows
    Update the memory of crows
    end while
```
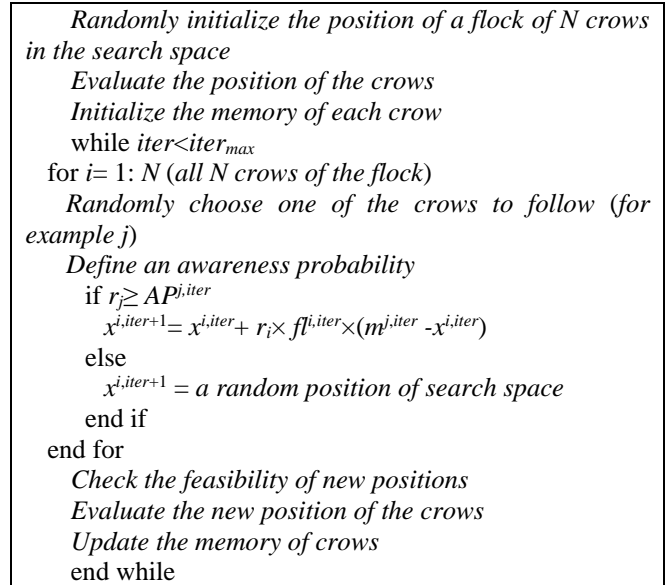
Fig. 5. CSA optimization algorithm pseudo-code [26].

Where r_i is a random number derived from uniform distribution between zero and one. $AP^{i,iter}$ also shows the probability of the *j*-th crow awareness in the *iter*-th iteration. By reducing the awareness probability parameter, the CSA algorithm directs the search process to the local search. On the other hand, by increasing the *AP* parameter, the overall search process is done, and a wider space will be searched. Therefore, in this condition, there is a population diversity and search space that prevents the early convergence of the algorithm. The pseudo-code of the CSA optimization algorithm is described in the Fig. 5. The implication of CSA and its position in the problem is illustrated in the flowchart of Fig. 6.
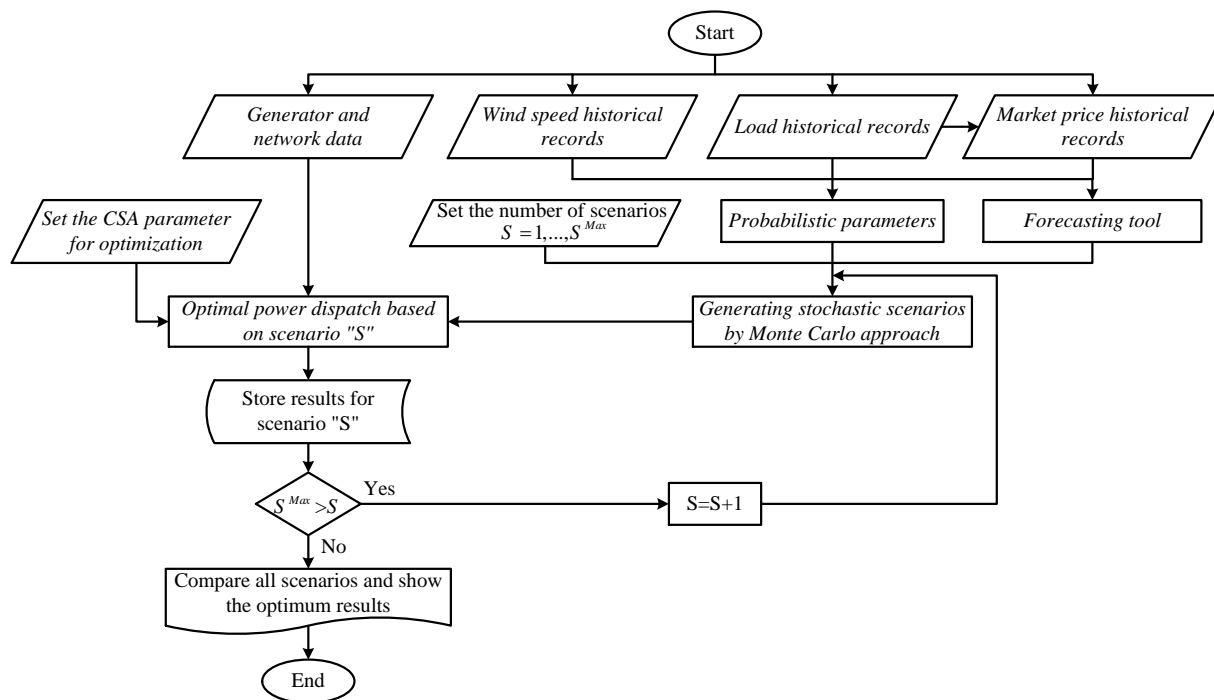
Fig. 6. The flowchart of simulation

6. Numerical Simulation and Results

The proposed algorithm has been developed for the optimal operation of a microgrid. The mean and the standard deviation of the microgrid's load, hourly market price, and the wind speed for the 24-hour period of the target day are shown in Table 1. The wind units are obliged to choose what to do while the time is approached the real-time operation and their more accurate prediction declares that they will have excess generation. In this case, they can have coordinated operation with ARES storage through hour-ahead transactions. Otherwise, they have two alternatives. They have to whether curtail the excess generation or sell it to the grid with a lower price due to the penalty factor which imposed by ISO for positive imbalances [27,28]. The latter is valid if it is legislated in the market structure rules. The technical characteristics of the wind turbine, the technical characteristics of the ARES storage unit, the connection capacity to the upstream network, and the economic characteristics of the microgrid's components are shown in Tables 2, 3, and 4 respectively. The interest rate is also considered 5%. The computer program is run by the 2017a MATLAB software via a 3.5 GHz processor and 16 GB of RAM at 145 seconds. The output power of the wind unit and the consumption of the microgrid's loads are shown in the Figs. 7 and 8 by considering the uncertainty using the Monte Carlo simulation which is performed with the implementation of the developed program with consideration of the energy market hourly price.

The purpose of this study is to investigate the optimal operation of a microgrid and the economical joint operation of wind and ARES units subject to maximize the profit of all units. In this respect, three scenarios are proposed as follows:

- Scenario 1: Establishing the operation schedule based on suppling from upstream network (without wind and ARES units)

- Scenario 2: Arrangement of the operation schedule based on supplying the grid from upstream network and wind farm.
- Scenario 3: Arrangement of the operation schedule based on supplying the grid from upstream network, wind farm and ARES unit.

Table 2. The characteristics of the wind power unit [29].

Rated Power	2 MW
Blade Quantity	3 Blades
Rotor Blade Diameter	110 m
V_{ci}	3 m/s
V_r	10 m/s
V_{co}	20 m/s
Temperature Range	-25°C ~ +50°C
Design Lifetime	25 Years

Table 3. Technical characteristics of the ARES unit [30]

Charging Capacity	57MW
Discharging Capacity	44MW
Storage Duration	15 min
Elevation Differential	2000
Average Grade	6.9%
Maximum Grade	8%
Track Length	5.5 mi.
Number of Trains	6
Row Size	72 acres
Ramp Rate	300 MW/min
System Life	40+ yrs.

Table 1. Historical data of the uncertainty parameters

Time (t)	Wind speed (m/s)		Load (MW)		Market price ($/MWh)	
	μ^t_{wind}	σ^t_{wind}	μ_L^t	σ_L^t	μ^t_{grid}	σ^t_{grid}
1	5.234	2.051	25.779	1.239	110	10
2	6.004	2.815	21.849	1.005	110	18
3	6.027	3.157	19.003	0.745	110	2
4	5.128	2.504	17.230	0.343	107	19.6
5	5.865	2.688	15.729	0.448	111	15.5
6	4.908	2.134	15.953	0.131	112	14
7	5.049	2.554	21.060	0.903	132	16.1
8	4.272	2.116	28.080	0.099	136	18.3
9	6.043	2.328	39.494	1.234	131	19.9
10	8.202	4.341	39.062	0.228	130	6.6
11	8.016	2.332	38.556	0.421	126	11.9
12	7.209	2.592	44.127	4.409	148	21.8
13	7.372	2.515	44.310	3.790	154	14.3
14	8.739	3.763	40.509	1.438	151	20.8
15	8.928	3.753	38.925	4.075	176	3.4
16	10.270	4.037	37.168	0.1713	174	2.5
17	10.128	4.195	36.750	1.672	183	6.2
18	8.882	4.151	50.596	2.714	244	6.2
19	7.210	3.753	65.023	8.981	235	4.7
20	6.840	2.465	71.203	11.427	244	31
21	6.192	3.312	73.501	2.803	183	17
22	8.342	4.268	64.321	5.712	154	21.9
23	6.365	3.002	55.858	3.848	145	4.2
24	5.779	2.880	40.004	2.907	112	12.2

Table 4. Economic characteristics of the microgrid components [29-30]

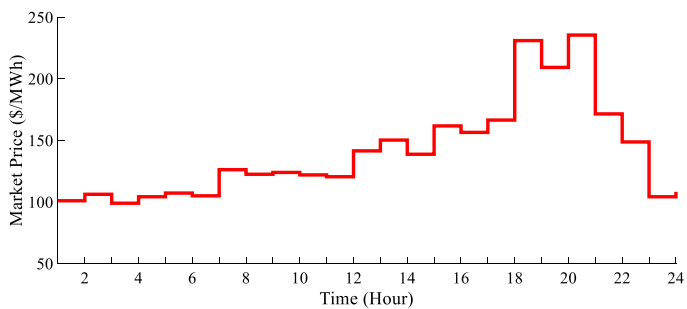| component	Lifetime (Year)	Initial investment cost ($/MW)	Capacity Factor (CF)	Repair and maintenance costs ($/Year)	Efficiency (%)
Wind Turbine	25	1519000	0.35	13200	50+
ARES	40+	1200000	0.85	14800	80+

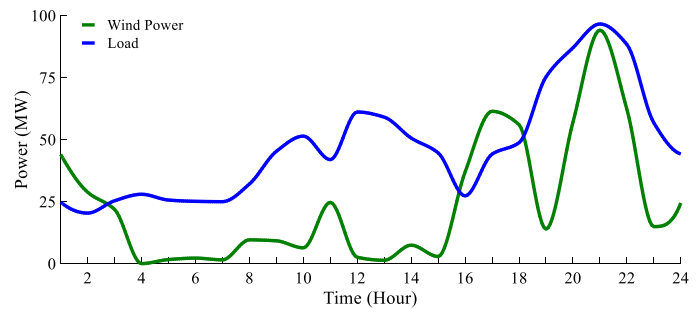**Fig. 7.** The hourly energy price in terms of uncertainty.

Fig. 8. The wind unit's output power and the microgrid load in terms of uncertainty.

In the first scenario, the whole of demand is supplied through the upstream network and the total operational cost is $170728. In this case, the average of operational costs is obtained 151.33 $/MWh.

In the second scenario, the wind farms are joined to the microgrid to supply the demand. According to Fig. 8, at hours 1-2 and 16-18, the generated power by wind farms exceeds from the demand of the grid. Hereby, the excess generation can be sold to the upstream network instead of curtailment. The total wind power generation is obtained 584.76 for the entire target day. The amount of 522.91 MW is dedicated to supplying the grid's loads, and the rest of wind generation (61.85 MW) are sold to the upstream network. In this case, the amount of purchased power from the upstream network, and the cost of purchased power are obtained 605.29 MW and $77760.64. The paid power by loads of microgrid to the wind farms is $84327, and the paid power to wind them by the upstream network is $6679.62. The operational cost of the 2nd scenario is $162088, which implies 5.33% cost reduction compared with the 1st scenario. This matter indicates the average cost of 143$/MWh for this scenario.

In the third scenario, ARES unit is joined to the microgrid to improve the performance of the system. In this case, a coordinated operation of wind and storage units for the microgrid is implemented subject to maximize their profit. Similar to the 2nd scenario, at hours 1-2 and 16-18, the generated power by wind farms exceeds from the demand of the grid. Hereby, part of the surplus wind generation is absorbed by ARES unit, and the rest of wind power is injected (sold) to the main grid. Similar to the scenario 2, the total wind power generation is 584.76 for a 24-hour period. This energy supplies the demand of 522.91 MW, and 20.67 MW is absorbed by the ARES unit. The rest of energy equal with 41.18 MW is sold to the upstream grid. The scheduling is executed so that the maximum profit is materialized for wind and ARSE unit. According to the schedule, the purchased energy from the main grid is $76499.43, the sold wind power to the grid's loads cost $84327.55. The profit of wind farm through selling excess power to the grid and ARES is $6892.43. The ARES unit has bought 34.8 MW within various hours (mainly off-peak) from the upstream network and the wind farm. It sells it back to the microgrid during peak hours when the electricity has higher prices. The ARSE unit has paid $3258.26 for its consumed power and has had the revenue of $6330.72. In this regard, the profit of $3072.45 is achieved by ARES unit. Therefore, the total operational cost of the system and the average operational cost are obtained $160826.98 and 142.55 $/MWh respectively. These results imply that the operational costs are mitigated in comparison with other two scenarios. Table 5 illustrates the results of the simulation of microgrid operation for all scenarios.

As can be noticed from proposed three scenarios, the coordinated operation of wind farm and storage unit will be led to the most cost reduction and consequently increase in wind farm profitability as an uncertain renewable source of generation as well as the profitability of cheap thermal units. Hence, the results of the 3rd scenario will be discussed in the following.

Table 5. The Microgrid's power exchanges and economic conditions in all scenarios

	Scenario 1	Scenario 2	Scenario 3
The bought power from the upstream network	1128.202	605.291	604.433
The total wind power generation	-	584.762	584.762
The sold wind power to the microgrid	-	522.911	522.911
The sold wind power to the upstream network	-	61.851	34.845
The sold power to ARES unit	-	-	20.668
The revenue of the upstream network from selling power to the microgrid	170728.267	77760.642	76499.426
The revenue of the wind farm from selling power to the microgrid	-	84327.553	84327.553
The revenue of the wind farm from selling power to the microgrid, upstream network and storage unit	-	91007.171	91219.979
The profit of ARES from selling electricity to the microgrid	-	-	3072.453
The total cost of operation	170728.267	162088.196	160826.979
The average cost of operation	151.327	143.669	142.551

Fig. 9 shows the energy exchange of the microgrid with the upstream network (buying and selling of power) where the orange bars represent the injected power of the microgrid from the connection bus to the grid and the pink bars stands for the absorbed power from the network to the microgrid. Fig. 10 shows the charge and discharge condition of the ARES unit. The microgrid sells power to the upstream network at 1 to 2 a.m., and 4 to 6 p.m., and 21 p.m., as it is shown in the Fig. 9. At 9 p.m., the generated power in the wind power unit is close to the consumed power of the microgrid, and the price of the energy market is at maximum, so the microgrid sells power to the upstream by utilizing the ARES. At 1 to 2 a.m., the generated power in the wind power unit is greater than the consumed load of the microgrid. Thus, the excess generated power by the wind unit during these hours is used to store in ARES at off-peak hours and to sell to the upstream network at peak hours. Hence, the more integration of renewable energy is achieved.
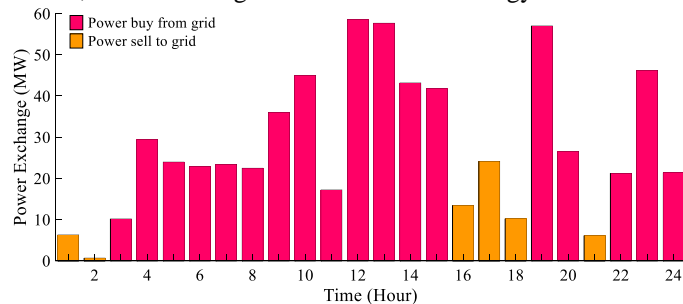

Fig. 9. The microgrid energy exchange with the upstream network (buying and selling of power).
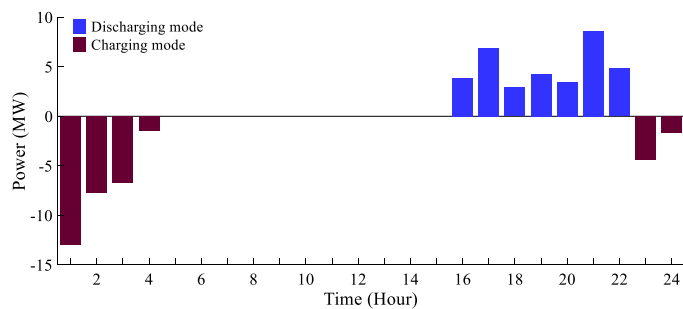
Fig. 10. Diagram of the ARES unit charge and discharge.

The analysis of the model's output data for 4 to 6 p.m. shows that the total amount of the microgrid's loads in these hours is 120.122 MW and the total amount of the wind unit generation is 154.321 MW. In these hours, ARES also generates 13.679 MW power, and the amount of sold power to the upstream network is 47.878 MW.
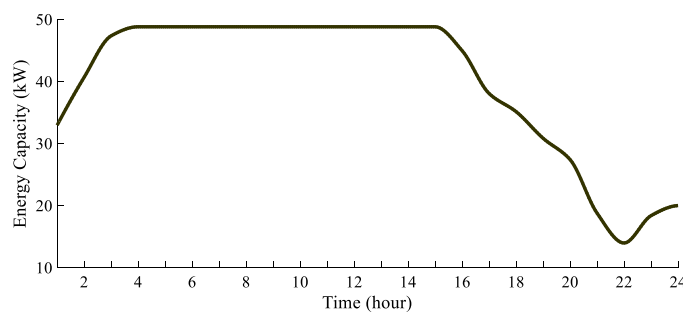

Fig. 11. Stored energy changes in ARES

The stored energy changes in ARES are shown in Fig. 11. As it can obviously be seen, the available energy in ARES is discharged to the minimum in order to maximize the profitability of the microgrid. It is also observed that during the hours when the price of the energy market has been high, ARES has operated in discharging mode, and the level of energy in the ARES has decreased. At times when the price of the energy market has been dropped, ARES operation was in charging mode, and the level of energy in the ARES increases. For example, between 1-4 a.m. and 10-12 p.m. that the energy market price is low, ARES has been operated in the charging mode, and the stored energy level in ARES has increased to 48.805 MW.

7. Conclusion

In this paper, a probabilistic method is employed to simulate the hourly microgrid operation with the inclusion of uncertainties of wind speed, electrical loads, and electricity price. The results clearly show the effectiveness of the proposed method. The employed CSA algorithm properly helps to achieve a near-optimal profit and determines the most appropriate operational status of each component in the microgrid. The amount of power exchange with the main grid and the charging/discharging state of ARES power plant for the day-ahead schedule is determined by the employment of CSA algorithm. In this study, three scenarios are proposed. In the first scenario, the demand of the grid will be satisfied from the main grid. In the second, the wind farm is joined to the grid. In the third, both wind farm and ARES unit have commitments in load satisfaction and have power exchange.

The results show that the third scenario has the best operational results and cost reduction and provide the most profitability for both wind farm and storage unit. The results denote that the operational costs of the system are $170728.267, $162088.196, and $160826.979 in the 1st, 2nd, and 3rd scenario respectively, which imply that the third scenario has the most cost reduction. The average cost of operation is 142.551 $/MWh in the third scenario. The revenue of the wind farm has increased up to $91219.979 by 1% for a 24-hour period. In addition, the ARES unit is profited by $3072.453 from its commitments in various hours.

References

[1] Hossain, E., Perez, R., & Bayindir, R. "Implementation of hybrid energy storage systems to compensate microgrid instability in the presence of constant power loads." In *Renewable Energy Research and Applications (ICRERA), 2016 IEEE International Conference on*, pp. 1068-1073. IEEE, 2016.

[2] Morel, J., Obara, S. Y., Sato, K., Mikawa, D., Watanabe, H., & Tanaka, T. "Contribution of a hydrogen storage-transportation system to the frequency regulation of a microgrid." In *Renewable Energy Research and Applications (ICRERA), 2015 International Conference on*, pp. 510-514. IEEE, 2015.

[3] Memar, M. R., Moazzami, M., Shahinzadeh, H., & Fadaei, D. "Techno-economic and environmental analysis of a grid-connected photovoltaic energy system." In *Electrical Power Distribution Networks Conference (EPDC), 2017 Conference on*, pp. 124-130. IEEE, 2017.

[4] Mane, S., Kadam, P., Lahoti, G., Kazi, F., & Singh, N. M. "Optimal load balancing strategy for hybrid energy management system in DC microgrid with PV, fuel cell and battery storage." In *Renewable Energy Research and Applications (ICRERA), 2016 IEEE International Conference on*, pp. 851-856. IEEE, 2016.

[5] Shahinzadeh, H., Moazzami, M., Fathi, S. H., & Gharehpetian, G. B. "Optimal sizing and energy management of a grid-connected microgrid using HOMER software." In *Smart Grids Conference (SGC), 2016*, pp. 1-6. IEEE, 2016.

[6] Naveed, S., Khan, S. M., & Najam-ul-Islam, M. "Techno-Economic Analysis of a Hybrid Grid-Connected/PV/Wind System in Pakistan." *International Journal of Renewable Energy Research (IJRER)* 6, no. 4 (2016): 1318-1327.

[7] Nadimi, A., & Adabi, F. "Optimized Planning for Hybrid Micro-grid in Grid-connected Mode." *International Journal of Renewable Energy Research (IJRER)* 6, no. 2 (2016): 494-503.

[8] Choi, J., Park, W. K., & Lee, I. W. "Application of vanadium redox flow battery to grid connected microgrid energy management." In *Renewable Energy Research and Applications (ICRERA), 2016 IEEE International Conference on*, pp. 903-906. IEEE, 2016.

[9] Hossain, E., Xahin, M. Z., Islam, K. R., & Akash, M. Q. "Design a Novel Controller for Stability Analysis of Microgrid by Managing Controllable Load using Load Shaving and Load Shifting Techniques; and Optimizing

Cost Analysis for Energy Storage System." *International Journal of Renewable Energy Research (IJRER)* 6, no. 3 (2016): 772-786.

[10] Zaman, F., Elsayed, S. M., Ray, T., & Sarker, R. A. "Evolutionary algorithms for power generation planning with uncertain renewable energy." *Energy* 112 (2016): 408-419.

[11] Mohammadi, S., Soleymani, S., & Mozafari, B. "Scenario-based stochastic operation management of microgrid including wind, photovoltaic, micro-turbine, fuel cell and energy storage devices." *International Journal of Electrical Power & Energy Systems* 54 (2014): 525-535.

[12] Jabbari-Sabet, R., Moghaddas-Tafreshi, S. M., & Mirhoseini, S. S. "Microgrid operation and management using probabilistic reconfiguration and unit commitment." *International Journal of Electrical Power & Energy Systems* 75 (2016): 328-336.

[13] Sobu, A., & Wu, G. "Optimal operation planning method for isolated micro grid considering uncertainties of renewable power generations and load demand." In *Innovative Smart Grid Technologies-Asia (ISGT Asia), 2012 IEEE*, pp. 1-6. IEEE, 2012.

[14] Shahinzadeh, H., Gheiratmand, A., Moradi, J., & Fathi, S. H. "Simultaneous operation of near-to-sea and off-shore wind farms with ocean renewable energy storage." In *Renewable Energy & Distributed Generation (ICREDG), 2016 Iranian Conference on*, pp. 38-44. IEEE, 2016.

[15] Fraleoni-Morgera, A., & Lughi, V. "Overview of Small Scale Electric Energy Storage Systems suitable for dedicated coupling with Renewable Micro Sources." In *Renewable Energy Research and Applications (ICRERA), 2015 International Conference on*, pp. 1481-1485. IEEE, 2015.

[16] Shahinzadeh, H., Gheiratmand, A., Fathi, S. H., & Moradi, J. "Optimal design and management of isolated hybrid renewable energy system (WT/PV/ORES)." In *Electrical Power Distribution Networks Conference (EPDC), 2016 21st Conference on*, pp. 208-215. IEEE, 2016.

[17] Medina, P., Bizuayehu, A. W., Catalão, J. P., Rodrigues, E. M., & Contreras, J. "Electrical energy storage systems: technologies' state-of-the-art, techno-economic benefits and applications analysis." In *System Sciences (HICSS), 2014 47th Hawaii International Conference on*, pp. 2295-2304. IEEE, 2014.

[18] Letcher, T. M., Law, R., & Reay, D. *Storing Energy: With Special Reference to Renewable Energy Sources*. Elsevier, 2016.

[19] http://s3.amazonaws.com/siteninja/multitenant/assets/21125/files/original/All_About_ARES_-_070616.pdf

[20] http://www.aresnorthamerica.com/ares-performance

[21] Shahinzadeh, H., Moazzami, M., Abbasi, M., Masoudi, H., & Sheigani, V. "Smart design and management of hybrid energy structures for isolated systems using biogeography-based optimization algorithm." In *Smart Grids Conference (SGC), 2016*, pp. 1-7. IEEE, 2016.

[22] Kotra, S., & Mishra, M. K. "Energy management of hybrid microgrid with hybrid energy storage system." In *Renewable Energy Research and Applications (ICRERA), 2015 International Conference on*, pp. 856-860. IEEE, 2015.

[23] Arriagada, E., Lopez, E., López, M., Blasco-Gimenez, R., Roa, C., & Poloujadoff, M. "A probabilistic economic dispatch model and methodology considering renewable energy, demand and generator uncertainties." *Electric Power Systems Research* 121 (2015): 325-332.

[24] Gal, N., Milstein, I., Tishler, A., & Woo, C. K. "Fuel cost uncertainty, capacity investment and price in a competitive electricity market." *Energy Economics* 61 (2017): 233-240.

[25] Mahdavi, M. S., Vahidi, B., & Gharehpetian, G. B. "A Novel Optimized Fuzzy Approach Based on Monte Carlo Method for System Load, Wind Turbine and Photovoltaic Unit Uncertainty Modeling in Unit Commitment." *Electric Power Components and Systems* 44, no. 8 (2016): 833-842.

[26] Askarzadeh, A. "A novel metaheuristic method for solving constrained engineering optimization problems: crow search algorithm." *Computers & Structures* 169 (2016): 1-12.

[27] Korpaas, M., Holen, A. T., & Hildrum, R. "Operation and sizing of energy storage for wind power plants in a market system." *International Journal of Electrical Power & Energy Systems* 25, no. 8 (2003): 599-606.

[28] Moradi, J., Shahinzadeh, H., Khandan, A., Moazzami, M., "A Profitability Investigation into the Collaborative Operation of Wind and Underwater Compressed Air Energy Storage Units in the Spot Market." *Energy* (2017), doi: 10.1016/j.energy.2017.11.088.

[29] https://www.vestas.com/en/products/turbines/v110%202_0_mw#

[30] http://www.aresnorthamerica.com/about-ares-north-america